Pressure-induced structural transformation of CdSe nanocrystals studied with molecular dynamics

X. Ye,[1] D. Y. Sun,[2] and X. G. Gong[1]
[1]*Key Laboratory of Surface and Department of Physics, Fudan University, Shanghai 200433, People's Republic of China*
[2]*Key Laboratory of Optical and Magnetic Resonance Spectroscopy and Department of Physics, East China Normal University, Shanghai 200062, People's Republic of China*
(Received 29 July 2007; published 10 March 2008)

We have studied the pressure-induced structural transformation of CdSe nanocrystals using constant pressure molecular dynamics simulations for finite system. We have observed the transformation from wurtzite to rocksalt structure, the process of transformation is strongly dependent on the shape and size of the nanocrystals, and transformation pressure decreases with increasing nanocrystal size. The spherical CdSe nanocrystals studied undergo nonuniform deformation, while the faceted ones undergo uniform deformation. The reverse transformation from rocksalt backward to wurtzite structure of the nanocrystals happens below 1 GPa at room temperature, and the width of the transformation decreases as the temperature increases.

DOI: 10.1103/PhysRevB.77.094108 PACS number(s): 61.50.Ks

I. INTRODUCTION

Pressure-induced structural transformation of group IV-IV, III-V, and II-VI compound semiconductors, such as GaN, SiC, ZnO, and CdSe, has been a longstanding topic of experimental and theoretical research. Experiments and theoretical studies have shown that this kind of compound semiconductor would undergo a transformation from fourfold coordinated structure [zinc blende (ZB) or wurtzite (WZ)] to sixfold coordinated rocksalt (RS) structure under hydrostatic pressure.[1–27] For example, the highly covalent ZB-type SiC starts to transform into RS at a pressure of ~100 GPa,[8,9] whrereas the less covalent WZ-type CdSe starts to transform at a much lower pressure of ~2 GPa.[10,11] While the transition pressure of these phase transformation has been studied extensively, the transformation mechanism is still on debate. One of the reasons is that transformations in bulk materials are dominated by growth mechanisms and have inherently irreproducible transition cycles due to the defects generated during the course of the transformation.[28]

As an intermediate system between single atoms and bulk material, semiconductor nanocrystals are also of experimental and theoretical interest. Compared with bulk material, nanocrystal behaves as single structural domains. Study of the nanocrystal would help us to understand the mechanism of the transformation which is hard to learn from bulk materials. Theoretical and experimental researches have shown that optical and electronic properties of nanocrystals are closely related to their mechanical and structural properties.[29] Thus, understanding the mechanisms of the structural transformations at the nanoscale would facilitate developing nanomaterials and devices.[30,31] Nanocrystals have quite different elastic and thermodynamic properties from their bulk counterparts because of the much higher surface to volume ratio. The CdSe nanocrystal system has been used as a model for structural studies. In the last few years, Alivisatos and co-workers have done a series of high pressure experiments on CdSe nanocrystals.[11,28,32–36] The results show that, similar to bulk material, CdSe nanocrystals would transform from fourfold coordinated WZ/ZB structure to a more densely packed sixfold coordinated RS structure with 18% reduction in volume under hydrostatic pressure, and the transformation is dependent on the size and shape of the nanocrystals. Recently, theoretical efforts have concerned with the possible mechanism and metastable structure of the transformation of CdSe nanocrystal changing from WZ to RS structure, a new intermediate structure for faceted CdSe nanocrystal during the transformation has been identified.[37] Although many experimental and theoretical efforts have been made to this area, the microscopic transformation mechanism from WZ to RS structure of CdSe at nanoscale has not been completely understood yet.[38–41] All these inspire us to investigate the pressure-driven transformation in nanocrystals of CdSe using the molecular dynamics approach.

In present paper, we report the results of molecular dynamics (MD) simulations of CdSe nanocrystals of various sizes and shapes undergoing forward and reverse structural phase transformations under hydrostatic pressure. We find the structural transformation of CdSe nanocrystal is highly affected by its size and shape. In the simulation, obvious hysteresis between the forward and backward transformations is observed. Upon transformation, grain boundaries are found for all spherical nanocrystals, while for the faceted ones, the general trend is to form single-domain structure.

II. COMPUTATIONAL DETAILS

The present study uses constant-pressure molecular dynamics method developed for finite systems.[42] We briefly outline this new method here, the details can be found in the original papers and recent review article.[42,43] In this method, the Lagrangian for a system is extended to include a PV term,

$$L_{extend} = \sum_{i}^{N} \frac{\mathbf{p}_i^2}{2m_i} - (\phi(\{\mathbf{r}_i\}) + P_{ext}V), \tag{1}$$

where $\mathbf{r}_i$, m_i, and $\mathbf{p}_i$ are the position, mass, momentum of the ith atom, respectively, ϕ is the interaction potential, and P_{ext}

and V are the external pressure and volume, respectively. Different from the Andersen–Parrinello–Rahman Car–Parrinello molecular dynamics method (APR-CPMD),[44,45] the volume in the new method is a function of atomic coordinations instead of a dynamics variable. The extended Lagrangian in the new method does not include a virtual kinetic energy and mass associated with the volume, which is presented in APR-CPMD. The equation of motion derived from above Lagrangian produces the constant pressure ensemble for the real systems, which can be obtained according to virial theorem.

$$\left\langle \frac{1}{3V}\left(\sum_i^N m_i v_i^2 - \sum_i^N \mathbf{r}_i \cdot \nabla_i \phi - \sum_i^N \mathbf{r}_i \cdot P_{ext} \nabla_i V \right) \right\rangle = 0, \tag{2}$$

where $\langle\ \rangle$ denotes average. Then, we have,

$$\left\langle \sum_i^N m_i v_i^2 - \sum_i^N \mathbf{r}_i \cdot \nabla_i \phi \right\rangle = \left\langle \sum_i^N \mathbf{r}_i \cdot P_{\text{ext}} \nabla_i V \right\rangle. \tag{3}$$

The key point of this method is to write the volume of systems as a function of atomic positions. Obviously, the volume can be written as a cubic homogeneous function of atomic positions. According to Euler theorem,

$$\sum_i^N \mathbf{r}_i \cdot \nabla_i V = 3V. \tag{4}$$

Finally, we end up with

$$P_{ext} = P_{int} = \left\langle \frac{1}{3V}\left(\sum_i^N m_i v_i^2 - \sum_i^N \mathbf{r}_i \cdot \nabla_i \phi \right) \right\rangle. \tag{5}$$

If the external pressure P_{ext} is a constant, P_{int} is also a constant. Thus, by writing the volume as a function of atomic coordinates, the constant-pressure MD can be achieved.

This new constant-pressure MD is parameter-free and can be used for any system with arbitrary shape in principle. This method is successfully used for the carbon nanotube systems.[46–50] In current calculations, the volume of the nanocrystals is calculated in the convex hull approximation. This approximations is based on finding the subset of atoms forming the smallest convex polyhedron. The QUICKHULL algorithm[52] was used to compute the convex hull of atomic configurations. Using this method, the current MD run does realize the constant-pressure ensemble. In Fig. 1, we have presented the pressure and volume as a function of simulation time. One can see that, in the simulation process, the internal pressure of systems dose have a constant value, and the volume fluctuates around its average value.

In the present study, most simulations are carried out at 300 K, where the system temperature is controlled by using a Nosé–Hoover thermostat.[51] The equations of motion are solved by using standard MD based on the Verlet-type algorithm. The time step is set as 2.0 fs. In order to study the effect of the surface structure on the transition mechanism, we use nanocrystals of two different shapes, consisting of 500–5000 atoms. The initial configuration of the spherical nanocrystal is cut out of bulk CdSe in WZ structure. Faceted

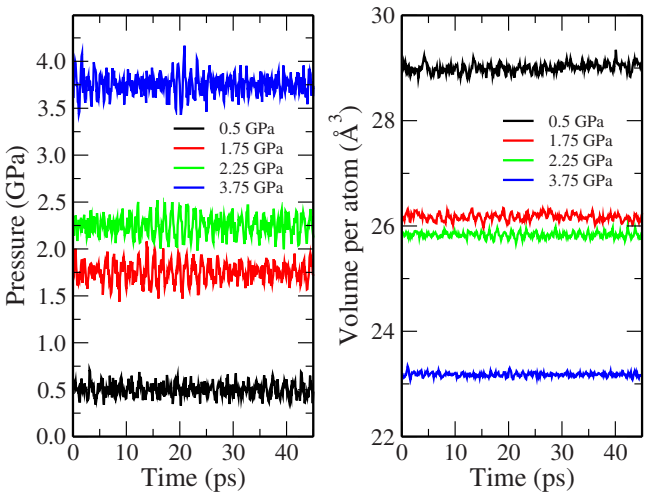

FIG. 1. (Color online) The internal pressure (left) and volume (right) as a function of the MD time for faceted $Cd_{1162}Se_{1162}$ nanocrystal. Both the pressure and volume of the system fluctuate around the average value.

nanocrystals with well-defined surface structure are obtained by cleaving the bulk lattice along equivalent (100) WZ planes and at (001) and $(00\bar{1})$ planes perpendicular to the [001] direction of the c axis. Before the pressure is applied to the CdSe nanocrystals, the crystal is relaxed for 30 ps at zero pressure. The pressure is increased from 0 GPa with pressure increasing in steps of 0.25 GPa until the structural transformation is completed, allowing 100 ps equilibration for each pressure increment, then the trajectories are collected for analysis. In all simulations, we use the empirical potential developed for CdSe by Rabani.[53] The potential is validated by comparing the computational results with experimental measurement for various physical properties, including lattice constant, elastic modulii, phonon dispersion, and the critical structural transformation pressure of bulk CdSe.

III. RESULTS AND DISCUSSIONS

The slope discontinuity of the volume-pressure relation clearly indicates the structural transformation of the CdSe nanocrystal under hydrostatic pressure. As shown in the left part of Fig. 2, the spherical $Cd_{502}Se_{502}$ nanocrystal volume decreases smoothly with increasing pressure up to a critical pressure (the pressure at which the WZ structure transforms to RS structure). At about 8.0 GPa, the volume decreases abruptly as a result of the transformation. This is in good agreement with the high pressure experiment.[34] However, for faceted nanocrystals, the behavior is somewhat different, as shown in the right part of Fig. 2. It can be seen an intermediate structure (C→D) exists between WZ and RS. This means that the faceted nanocrystals would experience structural changes twice before the whole transition process completely.

In order to quantitatively describe the transformation, we have calculated the variations of coordinations with pressure, as shown in Fig. 3. Here, those atoms are defined to be the

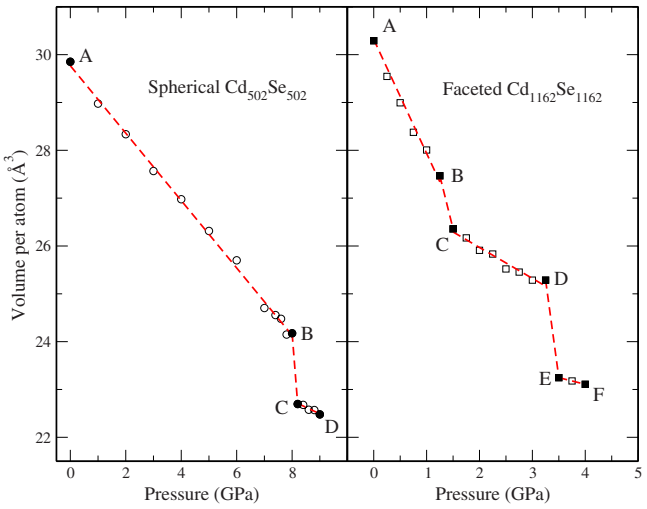

FIG. 2. (Color online) Volume versus pressure for faceted $Cd_{1162}Se_{1162}$ (right) and spherical $Cd_{502}Se_{502}$ nanocrystal (left). The discontinuity of the slopes indicates structural transformation under hydrostatic pressure.

nearest neighbors if the distance between them is less than 3.3 Å. From Fig. 3, we could see that at atmospheric pressure, besides fourfold coordinated atoms there are some threefold coordinated and fivefold coordinated atoms for spherical and faceted nanocrystals because of the initial defects at the nanocrystal surface. However, the fourfold coordinated atoms for the WZ structure account for nearly 70% of the nanocrystals. As the pressure increases, the number of fourfold coordinated atoms remains almost unchanged for a certain range of pressure, but the number of threefold coordinated atoms decreases and number of fivefold coordinated atoms increases slowly. Through analyzing the simulation runs by visual inspection, we find that with the enough pressure applied RS structure begins to nucleate at the surface for both spherical and faceted nanocrystals, while the inside part still remains perfect WZ structure, this coincides with that the structural transformation proceeds from surface to core of the nanocrystal with increasing pressure.[54] As the pressure continues to increase, as shown in the right part of Fig. 3, the number of fourfold atoms for faceted nanocrystals decreases sharply at about 1.4 GPa, and the number of the fivefold coordinated atoms increases very fast. It means that the faceted nanocrystal is experiencing some kind of structural transformation there.

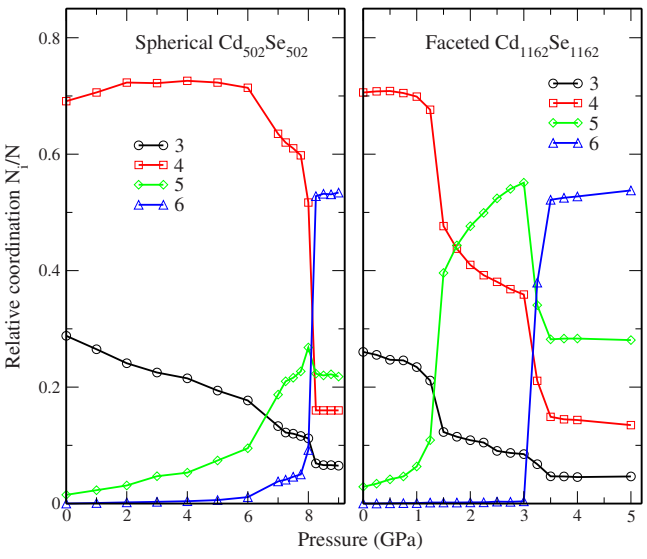

FIG. 3. (Color online) Relative coordination N_i/N versus pressure for spherical $Cd_{502}Se_{502}$ (left) and faceted $Cd_{1162}Se_{1162}$ (right). The coordination number is defined as the number of the nearest neighbor atoms.

From the snapshots of the MD simulation, we find the faceted nanocrystal transforms to a kind of fivefold coordinated structure by compressing in the *c* direction. This kind of fivefold coordinated structure has been reported as a stable phase of MgO under hydrostatic tensile loading.[39,55] However, for the CdSe faceted nanocrystal, this kind of structure is just metastable. When the pressure continues to increase, the fivefold coordinated structure transforms to sixfold coordinated RS structure. The fivefold coordinated to sixfold coordinated structural transformation is realized through changing of bond angle from 120° to 90° in the (001) plane, and the change is very fast. Similar transformation mechanism for faceted CdSe has been observed by Grünwald *et al.*[37] Their results show that the nanocrystal transformed from fourfold to fivefold coordinated structure very sharply and the structure can be stable for a certain range of pressure. However, our simulation reveals that the fourfold to fivefold coordinated structure transformation is a gradual process and the fivefold structure is metastable. This might explain why this structure cannot be observed in experiments. However, the spherical $Cd_{502}Se_{502}$ nanocrystal transforms from WZ structure to RS structure directly, as indicated by the sudden change from fourfold coordinated to sixfold coordinated structure in the left part of Fig. 3. Due to the symmetry, the spherical nanocrystal cannot be compressed in any special direction, such as the *c* axis of faceted nanocrystal.

We have also studied the reverse transformation of spherical CdSe nanocrystal. The structural transformation of CdSe nanocrystal can be reflected in the changes of bond angle distributions. The peaks around 108° and 90° correspond to WZ and RS phases respectively. The left part of Fig. 4 shows the case of increasing pressure applied on spherical nanocrystal $Cd_{502}Se_{502}$. It can be seen that at about 7.75 GPa, the peak at the value of 90° appears, indicating that the structure transformation occurs. At this pressure, both WZ and RS coexist. This is different from the experimental results. A too high pressure increasing step adopted in the experiment and a short time scale in the simulation might be the reason of such a disagreement. As the pressure increases to 8.25 GPa, the structure transforms to RS completed, as shown in the top left panel of Fig. 4. Upon pressure releasing, the transition is found to be highly hysteretic, as shown in the right part of Fig. 4. The rocksalt structure remains stable down to pressures significantly below the observed "upstroke" transition pressure. By about 0.5 GPa, however, the sample does begin to recover to WZ structure. By atmospheric pressure, the WZ is completely recovered. However, due to the structure defects, the surface structure can not be completely recovered. Meanwhile, we have investigated the transforma-

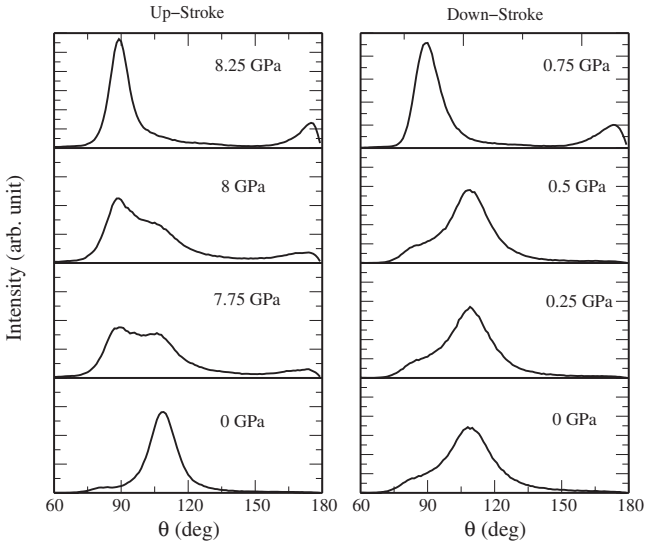

FIG. 4. Distribution of averaged bond angle of spherical $Cd_{502}Se_{502}$ nanocrystals. The left shows the increasing pressure process. The right shows the pressure decreasing process. With pressure decreasing to about 0.5 GPa, the transition from rocksalt to wurtzite structure occurs.

tion hysteresis as a function of temperature. Shown in Fig. 5, the width of the hysteresis decreases as the temperature increases. We could see that the upstroke transition pressure is very sensitive to the temperature, it decreases with increasing temperature, which is in good agreement with the experimental results.[34] As to the "downstroke" transition pressure, it will also be affected by the temperature. However, compared with the upstroke transition pressure, it is less sensitive to the temperature.

In addition, we have found that the transformation pressures are strongly dependent on the size of nanocrystals. The variation of the transformation pressure with spherical nanocrystal radius is shown in Fig. 6. The transformation pressure

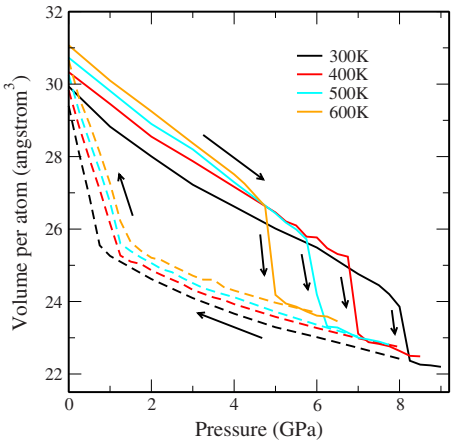

FIG. 5. (Color online) Hysteresis curves for the wurtzite structure to rocksalt structure transformation in spherical $Cd_{502}Se_{502}$ nanocrystal at different temperatures. Solid line for the increasing pressure process, while dash line for the decreasing pressure process. The hysteresis decreases with increasing temperatures.

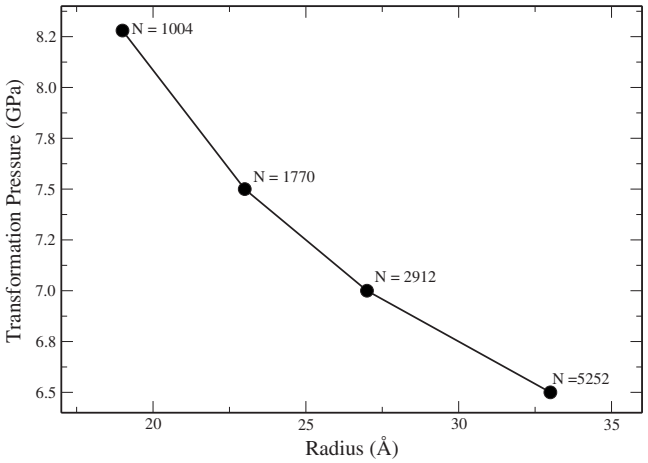

FIG. 6. Variation of the transformation pressure with radius for spherical nanocrystals at 300 K. With increasing nanocrystal size, the transformation pressure decreases.

decreases with increasing size (the critical transformation pressures are 8.25, 7.5, 7.0, and 6.5 GPa for nanocrystals with radii of 19, 23, 27, and 33 Å, respectively). This trend coincides with the experimental results of Tolbert and Alivisatos.[32,33] However, the values are somewhat higher than those of the experiments. One reason could be that the nanocrystals used in experiments were covered with surfactants, which strongly influenced surface energies. Such a surface passivation layer might lower the critical structural transformation pressure of the nanocrystals.

The volume compressibility of the nanocrystal can also be obtained directly from the simulation. Figure 7 shows the volume versus pressure for spherical $Cd_{502}Se_{502}$ nanocrystal. The data can be fitted with a linear volume compressibility of B_0=38.5 GPa for WZ structure and B_0=68.8 GPa for RS structure. The values are in good agreement with the results of the nanocrystal of comparable size from high pressure experiment. (The experimental values are 37 ± 5 and 74 ± 2 GPa for the comparable size of WZ and RS CdSe nanocrystals.[33])

One interesting phenomenon we want to address is that for all spherical nanocrystals studied here, nanoscale boundaries of different domains are found during and after the transformation. This is different from the experiments, where nanocrystals transform free of defects. In Fig. 8, grain boundaries are marked in gray. As the size of the nanocrystal increases, the multiple grains phenomena become more and more obvious. It has been pointed out above that the nanorystals in experiments are always passivated with organic ligands. Nanocrystals are not passivated in our simulations. Since the structural transformation is strongly affected by the surface structure, the passivation may be the key reason deciding whether the grain boundary exists. While for the faceted nanocrystals, the transformed structure is almost free of defects, which means that the structures display single-domain behavior. The reason could be related to the transformation mechanism because the transformation mechanism of faceted nanocrystals is simpler than that of spherical ones. As shown above, the faceted nanocrystal is compressed in

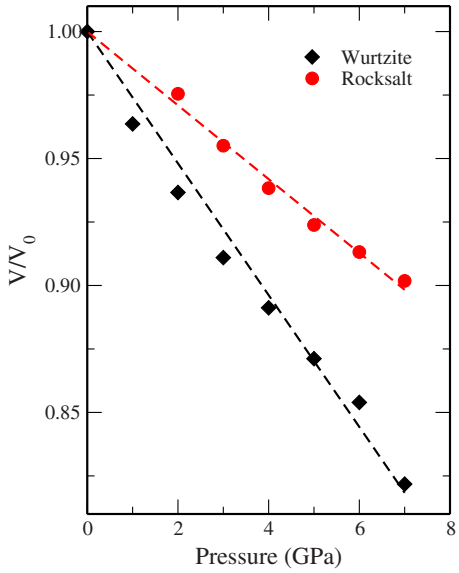

FIG. 7. (Color online) Unit cell volume versus external pressure for spherical $Cd_{502}Se_{502}$ nanocrystal. The black is for wurtzite structure with increasing pressure; the red is for rocksalt structure with decreasing pressure. The data can be fitted with a linear volume compressibility of B_0=38.5 GPa for wurtzite structure and B_0 =68.8 GPa for rocksalt structure.

the c direction first (WZ to fivefold coordinated structure), and then collapses in the (001) and $(00\bar{1})$ planes (fivefold coordinated structure to RS structure). This transformation in such order makes the transformed RS structure free from defects. Figure 9 shows the transformation process for faceted $Cd_{1162}Se_{1162}$ nanocrysal from fivefold coordination structure to rocksalt structure. It could be seen that the transformation of the faceted nanocrystal is a multinucleation process as spherical ones. During the fivefold coordinated to RS transformation, we have found some parts of the transformed RS structure changes back to the fivefold structure to avoid

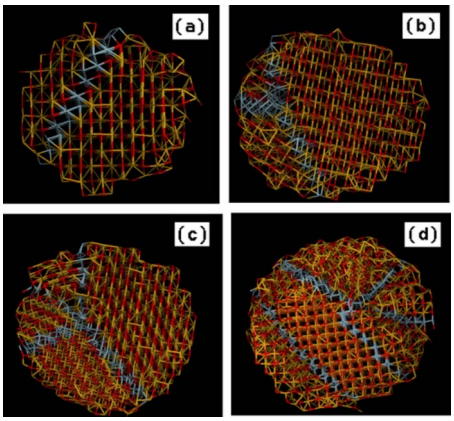

FIG. 8. (Color online) Domains after the structural transformation in spherical nanocrystals. (a), (b), (c), and (d) show the cross sections through the middle of the nanocrystals with radii of 19, 23, 27, and 33 Å, respectively. The grain boundaries are shown with gray atoms.

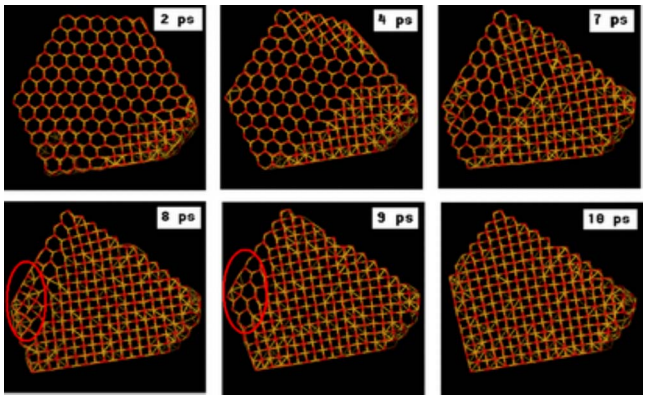

FIG. 9. (Color online) The snapshots of the MD simulation for the faceted $Cd_{1162}Se_{1162}$ nanocrysal transforming from fivefold coordination structure to rocksalt structure. The multinucleation phenomenon and rocksalt to fivefold structure backward transformation (the parts indicated by the red ellipse at 8 and 9 ps) could be clearly seen from the pictures.

forming a lattice defect. Alternatively, the whole nanocrystal could adjust the transformation path to achieve final perfect RS structure.

IV. SUMMARY

By using the constant-pressure molecular dynamics method specially developed for finite system, the structural transformation of CdSe nanocrystals under hydrostatic pressure is studied. We have found that the structural transformation of CdSe nanocrystal is highly affected by the size and shape. The results show that the pressure for WZ to RS structural transformation of spherical nanocrystal decreases with nanocrystal size. It is found that all spherical nanocrystals studied here undergo multiple grain deformation; grain boundary is formed in the transformed RS structure. Because all the faceted ones undergo uniform deformation, the transformed RS structure is of single domain nanocrystal. For the reverse transformation, the RS to WZ structure transformation of the nanocrystals always happens below 1 GPa at room temperature, and the width of the transformation hysteresis decreases as the temperature increases. Though our simulations show many similarities to actual experimental observation on CdSe nanocrystal, some difference still exists. The reason might be the passivation of the experimental samples. Therefore, the study of the surface passivation effects is an important issue to be considered in our future work.

ACKNOWLEDGMENTS

This research is partially supported by the National Science Foundation of China, the special funds for Major State Basic Research, MOE and Shanghai Project for the Basic Research. D.Y.S is also partially supported by Shanghai Municipal Education Commission and Shanghai Education Development Foundation. The computation is performed in the Supercomputer Center of Shanghai, the Supercomputer Center of Fudan University, and CCS.

[1] Y. N. Xu and W. Y. Ching, Phys. Rev. B **48**, 4335 (1993).
[2] J. K. Burdett and T. J. McLarnan, J. Chem. Phys. **75**, 5764 (1981).
[3] F. Shimojo, S. Kodiyalam, I. Ebbsjo, R. K. Kalia, A. Nakano, and P. Vashishta, Phys. Rev. B **70**, 184111 (2004).
[4] J. R. Chelikowsky and J. K. Burdett, Phys. Rev. Lett. **56**, 961 (1986).
[5] N. E. Christensen, S. Satpathy, and Z. Pawlowska, Phys. Rev. B **36**, 1032 (1987).
[6] P. Perlin, C. Jauberthie-Carillon, J. P. Itie, A. San Miguel, I. Grzegory, and A. Polian, Phys. Rev. B **45**, 83 (1992).
[7] H. Xia, Q. Xia, and A. L. Ruoff, Phys. Rev. B **47**, 12925 (1993).
[8] M. Yoshida, A. Onodera, M. Ueno, K. Takemura, and O. Shimomura, Phys. Rev. B **48**, 10587 (1993).
[9] T. Sekine and T. Kobayashi, Phys. Rev. B **55**, 8034 (1997).
[10] A. N. Mariano and E. P. Warekois, Science **142**, 672 (1963).
[11] J. N. Wickham, A. B. Herhold, and A. P. Alivisatos, Phys. Rev. Lett. **84** 923 (2000).
[12] M. D. Knudson, Y. M. Gupta, and A. B. Kunz, Phys. Rev. B **59**, 11704 (1999).
[13] S. Kodiyalam, R. K. Kalia, A. Nakano, and P. Vashishta, Phys. Rev. Lett. **93**, 203401 (2004).
[14] B. J. Morgan and P. A. Madden, Nano Lett.. **4**, 1581 (2004).
[15] D. Zahn, Y. Grin, and S. Leoni, Phys. Rev. B **72**, 064110 (2005).
[16] S. Limpijumnong and W. R. L. Lambrecht, Phys. Rev. Lett. **86**, 91 (2001).
[17] N. J. Lee, R. K. Kalia, A. Nakano, and P. Vashishta, Appl. Phys. Lett. **89**, 093101 (2006).
[18] S. Limpijumnong and S. Jungthawan, Phys. Rev. B **70**, 054104 (2004).
[19] M. S. Miao and Walter R. L. Lambrecht, Phys. Rev. B **68**, 092103 (2003).
[20] C. Molteni, R. Martonak, and M. Parrinello, J. Chem. Phys. **114**, 5358 (2001).
[21] M. Ueno, M. Yoshida, A. Onodera, O. Shimomura, and K. Takemura, Phys. Rev. B **49**, 14 (1994).
[22] M. Ueno, A. Onodera, O. Shimomura, and K. Takemura, Phys. Rev. B **45**, 10123 (1992).
[23] P. Perlin, C. Jauberthie-Carillon, J. P. Itie, A. San Miguel, I. Grzegory, and A. Polian, High Press. Res. **71**, 96 (1991).
[24] P. Perlin, I. Gorczyca, S. Porowski, T. Suski, N. E. Christensen, and A. Polian, Jpn. J. Appl. Phys., Suppl. **32**, 334 (1993).
[25] S. Uehara, T. Masamoto, A. Onodera, M. Ueno, O. Shimomura, and K. Takemura, J. Phys. Chem. Solids **58**, 2093 (1997).
[26] N. E. Christensen and I. Gorczyca, Phys. Rev. B **50**, 4397 (1994).
[27] A. Munoz and K. Kunc, Phys. Rev. B **44**, 10372 (1991).
[28] K. Jacobs, D. Zaziski, E. C. Scher, A. B. Herhold, and A. P. Alivisatos, Science **293**, 1803 (2001).
[29] B. B. Karki and R. M. Wentzcovitch, Phys. Rev. B **68**, 224304 (2003).
[30] H. Zhang, B. Gilbert, F. Huang, and J. F. Banfield, Nature (London) **424**, 1025 (2003).
[31] S. Vemparala, R. K. Kalia, A. Nakano, and P. Vashishta, J. Chem. Phys. **121**, 5427 (2004).
[32] S. H. Tolbert and A. P. Alivisatos, Science **265**, 373 (1994).
[33] S. H. Tolbert and A. P. Alivisatos, J. Chem. Phys. **102**, 4642 (1995).
[34] C.-C. Chen, A. B. Herhold, C. S. Johnson, and A. P. Alivisatos, Science **276**, 398 (1997).
[35] K. Jacobs, J. Wickham, and A. P. Alivisatos, J. Phys. Chem. B **106**, 3759 (2002).
[36] D. Zaziski, S. Prilliman, E. C. Scher, M. Casula, J. Wickham, S. M. Clark, and A. P. Alivisatos, Nano Lett. **4**, 943 (2004).
[37] Michael Grünwald, Eran Rabani, and Christoph Dellago, Phys. Rev. Lett. **96**, 255701 (2006).
[38] S. M. Sharma and Y. M. Gupta, Phys. Rev. B **58**, 5964 (1998).
[39] S. Limpijumnong and W. R. L. Lambrecht, Phys. Rev. B **63**, 104103 (2001).
[40] H. Sowa, Acta Crystallogr., Sect. A: Found. Crystallogr. **57**, 176 (2001).
[41] M. Wilson and P. A. Madden, J. Phys.: Condens. Matter **14**, 4629 (2002).
[42] D. Y. Sun and X. G. Gong, J. Phys.: Condens. Matter **14**, L487 (2002); arXiv:cond-mat/0102184 (unpublished).
[43] D. Y. Sun and X. G. Gong, arXiv:0802.0067 (unpublished).
[44] H. C. Andersen, J. Chem. Phys. **72**, 2384 (1980).
[45] M. Parrinello and A. Rahman, J. Appl. Phys. **52**, 7182 (1981); Phys. Rev. Lett. **45**, 1196 (1980).
[46] D. Y. Sun, D. J. Shu, M. Ji, Feng Liu, M. Wang, and X. G. Gong, Phys. Rev. B **70**, 165417 (2004).
[47] X. Ye, D. Y. Sun, and X. G. Gong, Phys. Rev. B **72**, 035454 (2005).
[48] X. Ye, D. Y. Sun, and X. G. Gong, Phys. Rev. B **75**, 073406 (2007).
[49] W. Yang, R. Z. Wang, Y. F. Wang, X. M. Song, B. Wang, and H. Yan, Phys. Rev. B **76**, 033402 (2007).
[50] J. Zang, A. Treibergs, Y. Han, and F. Liu, Phys. Rev. Lett. **92**, 105501 (2004).
[51] S. Nosé, Mol. Phys. **52**, 255 (1984); W. G. Hoover, Phys. Rev. A **31**, 1695 (1985).
[52] C. B. Barber, D. P. Dobkin, and H. Huhdanpaa, ACM Trans. Math. Softw. **22**, 469 (1996).
[53] E. Rabani, J. Chem. Phys. **116**, 258 (2002).
[54] S. Kodiyalam, R. K. Kalia, H. Kikuchi, A. Nakano, F. Shimojo, and P. Vashishta, Phys. Rev. Lett. **86**, 55 (2001).
[55] A. J. Kulkarni, M. Zhou, K. Sarasamak, and S. Limpijumnong, Phys. Rev. Lett. **96**, 105502 (2006).